Publications of the Korean Astronomical Society
32: 157 ∼ 161, 2017 March

pISSN 1225-1534
eISSN 2287-6936
https://doi.org/10.5303/PKAS.2017.32.1.157

AKARI OBSERVATIONS OF DUSTY TORI OF ACTIVE GALACTIC NUCLEI

Shinki Oyabu[1], Hidehiro Kaneda[1], Masaya Izuhara[1], Keisuke Tomita[1], Daisuke Ishihara[1], Kimiaki Kawara[2], and Yoshiki Matsuoka[3]

[1]Department of Physics, Graduate School of Science, Nagoya University, Furo-cho, Chikusa-ku, Nagoya, Aichi, 464-8602, Japan
[2]Institute of Astronomy, the University of Tokyo, 2-21-1 Osawa, Mitaka, Tokyo, 181-0015, Japan
[3]National Astronomical Observatory of Japan, 2-21-1 Osawa, Mitaka, Tokyo 181-8588, Japan

E-mail: oyabu@u.phys.nagoya-u.ac.jp

(Received February 20, 2016; Revised October 20, 2016; Accepted October 20, 2016)

ABSTRACT

The dusty torus of Active Galactic Nuclei (AGNs) is one of the important components for the unification theory of AGNs. The geometry and properties of the dusty torus are key factors in understanding the nature of AGNs as well as the formation and evolution of AGNs. However, they are still under discussion. Infrared observation is useful for understanding the dusty torus as thermal emission from hot dust with the dust sublimation temperature ($\sim$ 1500 K) has been observed in the infrared. We have analyzed infrared spectroscopic data of low-redshift and high-redshift quasars, which are luminous AGNs. For the low-redshift quasars, we constructed the spectral energy distributions (SEDs) with AKARI near-infrared and Spitzer mid-infrared spectra and decomposed the SEDs into a power-law component from the nuclei, silicate features, and blackbody components with different temperatures from the dusty torus. From the decomposition, the temperature of the innermost dusty torus shows the range between 900−2000 K. For the high-redshift quasars, AKARI traced rest-frame optical and near-infrared spectra of AGNs. Combining with WISE data, we have found that the temperature of the innermost dusty torus in high redshift quasars is lower than that in typical quasars. The hydrogen Hα emission line from the braod emission line region in the quasars also shows narrow full width at half maximum of 3000−4000 km s^{-1}. These results indicate that the dusty torus and the broad emission line region are more extended than those of typical quasars.

Key words: Quasars — Galaxies:active — Infrared:galaxies

1. INTRODUCTION

An Active Galactic Nucleous (AGN) is the centeral part of a galaxy with luminosity as high as a typical entire galaxy. The huge luminosity from an AGN is believed to be a result of the accretion of mass by a supermassive black hole (SMBH) at the centeral part of the host galaxy. There are gas clouds surrounding the accretion disk and they are the origin of broad emission lines. In addition to these components, there is a dusty torus surrounding the SMBH, the accretion disk and the gas clouds. The dusty torus plays important roles in the AGN. At first, it helps to develop the unified scheme. A single type of physical object observed under different line of sight can explain the different observational classes of AGNs, because a dusty torus is sometimes obstacle to see a central engine. The dusty torus is also a main contributor of infrared emission and represents the gas supply for the AGN. It is probable that the strong radiation affects the host galaxy evolution, and thus the presence and structure of a dusty torus might change the radiation effect on the host galaxy.

There are many observations of dusty torii. Especially quasars, which are luminous AGN, are well ob-

served due to their apparent brightness. Near-infrared spectroscopic observations reveal that the temperatures of a dusty torus is near the sublimation temperature of silicate grains (Kobayashi et al., 1993; Glikman et al., 2006). Spitzer observations (Mor et al., 2009; Mor & Netzer, 2012) suggest the presence of hotter-dust component in quasars. The hotter-dust component is associated with graphite located closer to the central engine, as graphite has a higher sublimation temperature than silicate. Interferometry and reverberation mapping observations show that the innermost size of dusty torus determined by sublimation of dust grain is smaller than a few parsecs (Suganuma et al., 2006; Kishimoto et al., 2011). For high-redshift quasars, observations with Infrared Space Observatory, AKARI, and Spitzer revealed the presence of hot dust, which indicates that the nuclear structures are already in place at high redshift. Further, they pointed out that there is the remarkable similarity in the rest frame near-infrared properties with their lower-redshift analogs (e.g. Oyabu et al., 2001, 2007, 2009; Hines et al., 2006; Jiang et al., 2006, 2010).

However, the nature and the evolution of the dusty torus are still not clear because the rest frame torus emission occurs in the near- and mid-infrared (which can be redshifted to longer wavelengths). Hence, we performed AKARI data analysis for the study of dusty torii in low- and high-redshift quasars to reveal the nature and the evidence of their evolution.

2. SAMPLE SELECTION AND DATA ANALYSIS

2.1. Hot-dust properties of low redshift quasars

In order to investigate structure of the dust torus, we have constructed spectral energy distributions (SEDs) of low-redshift quasars. Our sample of the low-redshift quasars consists of quasars observed with the AKARI IRC and Spitzer IRS at the wavelength of 2.5−5 μm and 5.2−36 μm, respectively. While 81 quasars satisfy the criterion, 32 quasars out of 81 are selected as high quality data.

The spectra constructed with AKARI IRC near-infrared and Spitzer IRS mid-infrared data cover the wavelength range between 2.5 μm and 36 μm in the observed frame. In addition, the SDSS optical and 2MASS near-infrared photometric data are combined. As a result, we have constructed spectral energy distributions of the sample quasars in the wavelength from 0.3 μm to 36 μm. Their spectra show polycyclic aromatic hydrocarbon (PAH) features at 3.3, 7.7, 8.6, 11.3, and 12.7 μm. We assume that the PAH features are associated with star-forming activities in host galaxies. Therefore, we subtracted a spectrum template of a star-forming galaxy, M82, from the spectra. The scaling factor of the M82 template was adjusted to subtract the PAH 7.7 feature. Figure 1 shows a spectrum of the quasar, PG 1512+370, after the M82 template are subtracted from the original spectra.

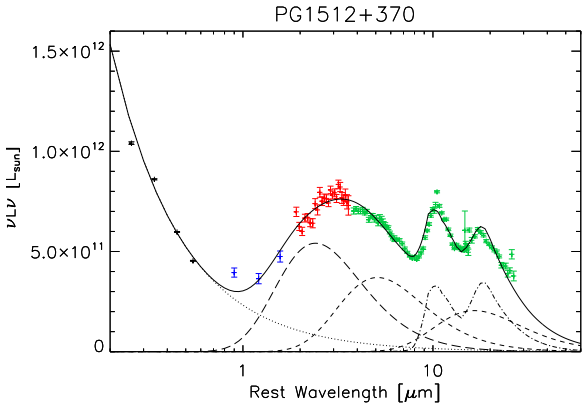

Figure 1. The spectral energy distribution of PG 1512+370. A power-law component and blackbodies are shown by a dotted line and dashed lines, respectively. A dot-dashed line shows a model of silicate features.

We fit the quasar spectra with the SED model consisting of five components: a power-law continuum in the UV/optical mainly representing emission from the accretion disk, silicate features which is the product of a blackbody and the silicate opacity (Laor & Draine, 1993), and three blackbodies from hot, warm, and cool dust components. Figure 1 also shows the fitted result.

2.2. Hot-dust emission and Hα emission line in high redshift quasars

Four luminous quasars at z=4.2−5.2, BR J0419−5716, BR J0529−3552, SDSS J1626+2751, and BR 2237−0607, are selected as our high-redshift sample. For high-redshift quasars, AKARI near-infrared spectra at 2.5−5 μm present the continuum emission from an accretion disk and a hydrogen Hα emission line from broad emission line region. In addition, we used the 9 μm images which were taken with one of the mid-infrared channels in the AKARI/IRC during the near-infrared prism spectroscopy. The 9 μm image provides the photometry around the rest-frame 1.5 μmin the spectrum. We constructed the SEDs of the quasars, compiling the WISE photometry data of these quasars at 3.4, 4.6, 12, and 22 μm.

Figure 2 shows an example of the SED of BR J0419-5716 at z=4.46. The AKARI near-infrared spectrum

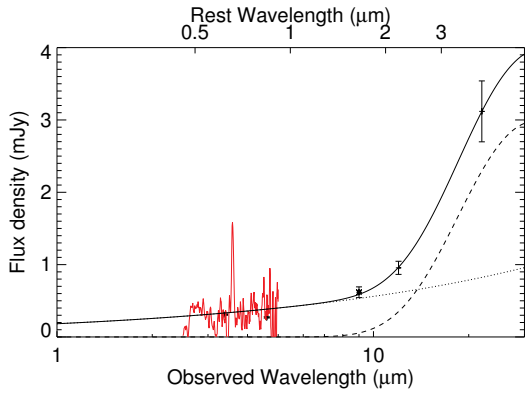

Figure 2. The near-infrared spectrum and photometry data of BR J0419-5716 at z=4.46. A solid line represents a continuum model cossist of a power-law (a dotted line) and a Blackbody (a dashed line) components.

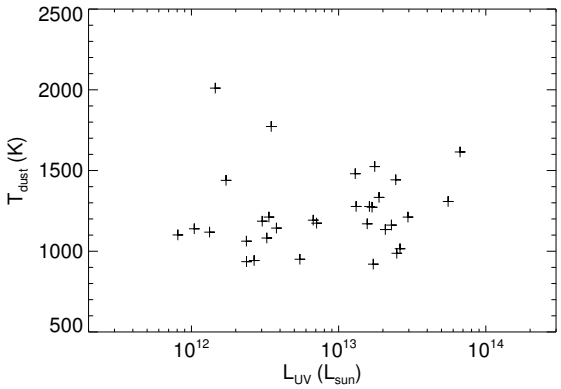

Figure 3. Temperatures of hot dust as a function of UV luminosity in low-redshift quasars.

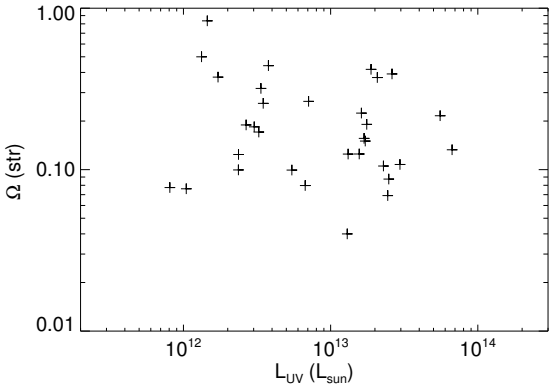

Figure 4. Solid angles of dusty torus as a function of UV luminosity in low-redshift quasars.

clearly detected the Hα emission line at an observed wevelength of 3.59 μm and the continuum from the accretion disk. Photometric data at 9, 12, 22 μm show the bump sharply rising at $\lambda > 9$ μm from a hot-dust component of the dusty torus. In order to measure the dust temperature, the model fitting to the SEDs is also performed. As shown in Figure 2, in the model, we reproduced the continuum by two components: a power-law continuum and a single-temperature blackbody. The measurement of the emission line is also performed by fitting a linear function to the local continuum and a Gaussian function to the emission line.

3. RESULTS

3.1. The structure of innermost dusty torus in low-redshift quasars

As a result of infrared spectral decompositions of low-redshift quasars, we have found that the temperature of the hot-dust component is 900−2000 K. Figure 3 shows the dust temperature as a function of the UV luminosity estimated from the fitting result of a power-law component. There is no correlation between the dust temperatures and the UV luminosity.

Using the hot-dust temperature and the distance between the nuclear and the innermost dusty torus, we have estimated the solid angles that the dusty torus covers around the nuclear source. The distances between the nuclear and the dusty torus are estimated to be 0.5-9 pc from the temperatures and the UV luminosity. Figure 4 shows the solid angles as a function of the UV luminosity. The solid angles are small, about 0.04−1 steradians, and there is no correlation between the solid angles and the UV luminosity, while Hasinger (2008) and Toba et al. (2014) have reported on the anti-correlation of the covering factors of the dusty torus, corresponding to the solid angles, on the X-ray and mid-infrared luminosity of quasars, respectively. The reason of this discrepancy is due to the luminosity difference. We have selected more luminous quasars than Hasinger (2008) and Toba et al. (2014). In addition, our result of small solid angles can be explained with the large luminosity of our sample quasars.

3.2. Dusty torus in high-redshift quasars

As a result of the SED fitting in the high-redshift quasars, we have found that the temperatures of the dusty torus in three quasars out of four is < 900 K. The temperatures are lower than the typical values of 900−2000 K which are estimated in the low-redshift quasars in this work. However, for one remaining quasar with the temperature of the dusty torus below 1300 K, we are not confident that the temperature of the dusty torus is below 900 K.

Our previous work shows that the quasar at similar redshift, APM 08279+5255, has the hot-dust component of 1300 K that is a typical value of quasars at low redshift (Oyabu et al., 2009). Our high-redshift quasars have the dusty torus of lower temperature (<900 K) than APM 08279+5255, which simply indicates that the dusty torus is extended farther from the nucleus than quasars with a typical dust temperature.

In order to understand the difference of the hot-dust temperature, the other properties of quasars are investigated. We have found that the full width at half maximum (FWHM) of the Hα emission line is lower than 4000 km s^{-1} for the high-redshift sample compared to the 7700 km s^{-1} of APM 08279+5255. The fact that the FWHMs of the Hα emission line are narrow suggests two possibilities; one is a less massive black hole, and the other is a large broad emission line region. By estimating the SMBH masses with the line luminosity and the FWHMs of the Hα emission line (Greene & Ho, 2005), the SMBH masses of our high-redshift quasar sample and APM 08279+5255 are $2-7\times10^9$ M$_\odot$, indicating that these quasars have similar SMBH masses. Therefore, we conclude that producing narrow FWHMs of the Hα emission lines in the high-redshift quasars are due to the large broad emission line region.

4. DISCUSSION

Even by considering the uncertainties three quasars in the low-redshift sample show the hot-dust temperature of $>$ 1500 K, which is the sublimation temperature of the silicate grain. AKARI spectra at the wavelength 2.5−5.0 μm are useful to reveal hot-dust temperature. Such hot dust with the temperature higher than 1500 K is reported by the Spitzer observations of low-redshift quasars (Mor et al., 2009; Mor & Netzer, 2012), and they suggest that the dust composition of graphite can be explained the dust temperature because graphite can survive at the temperature up to 1800 K.

At least, three quasars in our high-redshift sample have the dust temperature of $<$ 900 K and have the dusty torus extended beyond the typical radius between the nucleus and the innermost dust. On the other hand, the broad emission line region is also extended by measuring the FHWMs of the Hα emission line. Combining these results, these quasars are likely to be on the evolution stage of quasars when the components of gas and dust are gathering around the nucleus.

Figure 5 shows the hot-dust temperatures versus FHWMs of the Hα emission line. At low redshift, the hot-dust temperature is almost independent of the FWHMs of the Hα emission line, whereas the quasars with narrow FWHMs of the Hα emission line at high redshift tend to have the dusty torus with the temperature lower than those of low-redshift quasars. The quasars with narrow FWHMs at z$\sim$4−5 may be different from low-redshift quasars in the hot-dust temperature. This trend is derived from a small sample; larger samples are therefore needed for further statistical confirmation.

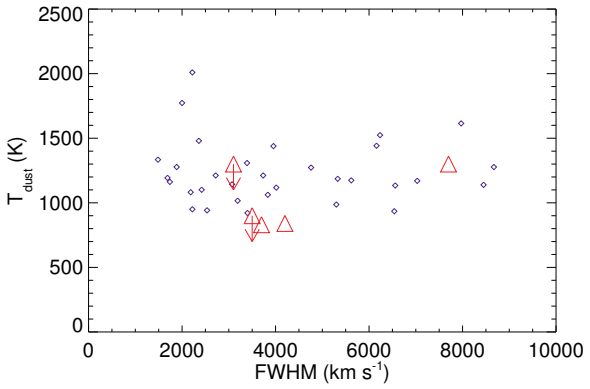

Figure 5. Dust temperature versus FWHM of Hα line. Diamonds and triangles indicate the low-redshift quasar and high-redshift quasar samples, respectively. High-redshift quasar sample consists of four quasars at z=4.2−5.2 in this work and APM 08279+5255 from Oyabu et al. (2009).

ACKNOWLEDGMENTS

This research is based on observations with AKARI, a JAXA project with the participation of ESA.

REFERENCES

Glikman, E., Helfand, D. J., & White, R. L., 2006, A Near-Infrared Spectral Template for Quasars, ApJ, 640, 579

Greene, J. E. & Ho, L. C., 2005, Estimating Black Hole Masses in Active Galaxies Using the Halpha Emission Line, ApJ, 630, 122

Hasinger, G,. 2008, Absorption properties and evolution of active galactic nuclei, A&A, 490, 905

Hines, D. C., Krause, O., Rieke, G. H., et al., 2006, ApJL, Spitzer Observations of High-Redshift QSOs, 641, L85

Jiang, L., Fan, X., Hines, D. C., et al., 2006, AJ, Probing the Evolution of Infrared Properties of z $\sim$ 6 Quasars: Spitzer Observations, 132, 2127

Jiang, L., Fan, X., Brandt, W. N., et al., 2010, Dust-free quasars in the early Universe, Nature, 464, 380

Kishimoto, M., Hönig, S. F., Antonucci, R., et al., 2011, The innermost dusty structure in active galactic nuclei as probed by the Keck interferometer ,A&A, 527, A121

Kobayashi, Y., Sato, S., Yamashita, T., Shiba, H., & Takami, H., 1993, An infrared study of hot dust in quasars using prism spectrophotometry, ApJ, 404, 94

Laor, A. & Draine, B. T., 1993, Spectroscopic constraints on the properties of dust in active galactic nuclei, ApJ, 402, 441

Mor, R., Netzer, H., & Elitzur, M., 2009, Dusty Structure Around Type-I Active Galactic Nuclei: Clumpy Torus Narrow-line Region and Near-nucleus Hot Dust, ApJ, 705, 298

Mor, R. & Netzer, H., 2012, Hot graphite dust and the infrared spectral energy distribution of active galactic nuclei, MNRAS, 420, 526

Oyabu, S., Kawara, K., Tsuzuki, Y., et al., 2001, ISO continuum observations of quasars at z=1-4. I. Spectral energy distributions of quasars from the UV to far-infrared, A&A, 365, 409

Oyabu, S., Wada, T., Ohyama, Y., et al., 2007, Detection of an Halpha Emission Line on a Quasar, RX J1759.4+6638, at z = 4.3 with AKARI, PASJ, 59, 497

Oyabu, S., Kawara, K., Tsuzuki, Y., et al., 2009,AKARI Near- and Mid-Infrared Spectroscopy of APM 08279+5255 at z = 3.91, ApJ, 697, 452

Suganuma, M., Yoshii, Y., Kobayashi, Y., et al., 2006, Reverberation Measurements of the Inner Radius of the Dust Torus in Nearby Seyfert 1 Galaxies, ApJ, 639, 46

Toba, Y., Oyabu, S., Matsuhara, H., et al., 2014, Luminosity and Redshift Dependence of the Covering Factor of Active Galactic Nuclei viewed with WISE and Sloan Digital Sky Survey, ApJ, 788, 45